J Pharm Biopharm Res, 2022, 4(1): 283-295
DOI: 10.25082/JPBR.2022.02.001

RESEARCH ARTICLE

Effect of experimental hyperglycemia on intestinal elimination and biliary excretion of ibuprofen enantiomers in hyperglycemic rats

Hawsar Othman Mohammed[1,2] **Attila Almási**[1] **Pál Perjési**[1*]

[1] Institute of Pharmaceutical Chemistry, Faculty of Pharmacy, University of Pécs, Pécs, Hungary
[2] College of Veterinary Medicine, University of Sulaimani, Sulaymaniyah, Kurdistan Region, Iraq

Correspondence to: Pál Perjési, Institute of Pharmaceutical Chemistry, Faculty of Pharmacy, University of Pécs, H-7624 Pécs, Hungary;
Email: pal.perjesi@gytk.pte.hu

Received: September 3, 2022;
Accepted: October 1, 2022;
Published: October 4, 2022.

Citation: Mohammed HO, Almási A and Perjési P. Effect of experimental hyperglycemia on intestinal elimination and biliary excretion of ibuprofen enantiomers in hyperglycemic rats. *J Pharm Biopharm Res*, 2022, **4**(2): 283-295.
https://doi.org/10.25082/JPBR.2022.02.001

Abstract: Diabetic complications are mostly due to hyperglycemia. Hyperglycemia is reported to be associated with oxidative stress. It can result in changes in the activities of drug-metabolizing enzymes and membrane-integrated transporters, which can modify the fate of drugs and other xenobiotics. An *in vivo* intestinal perfusion model was used to investigate how experimental hyperglycemia affects intestinal elimination and biliary excretion of ibuprofen enantiomers in the rat. Experimental diabetes was induced by intravenous (i.v.) administration of streptozotocin. The intestinal perfusion medium contained 250 μM racemic ibuprofen. A validated isocratic chiral HPLC method with UV detection was developed to determine the amount of the two enantiomers in the intestinal perfusate and the bile. The results indicated that experimental diabetes doesn't cause a statistically significant difference in the disappearance of ibuprofen enantiomers from the small intestine. Analysis of the bile samples detected only the (*S*)-IBP enantiomer. Excretion of the ibuprofen enantiomer to the bile decreased in experimental diabetes. The observed changes can affect the pharmacokinetics of drugs administered in hyperglycemic individuals.

Keywords: streptozotocin, hyperglycaemia, (*S*)-ibuprofen, biliary excretion

1 Introduction

Ibuprofen (IBP) (Figure 1(A)) is a non-steroidal anti-inflammatory drug (NSAID) belonging to the group of 2-arylpropionic acids (Figure 1) [1]. The molecule carrying a center of symmetry is used in therapy in racemic form, exploiting its three main pharmacological effects (anti-inflammatory, analgesic, and antipyretic). It is most commonly used in therapy by oral administration. After oral absorption, about 40–60% of the *R*(-)-form of ibuprofen is metabolically converted to the *S*(-) form [2, 3] in the intestinal tract and liver [4, 5]. Over 70% of the ibuprofen dose is metabolized and excreted in the urine. The major route of metabolism is CYP-catalyzed oxidative transformations resulting in the formation of hydroxyl-substituted ibuprofen metabolites. Ibuprofen and its oxidized metabolites were reported to form glucuronide conjugates excreted in the feces or the urine [6, 7].

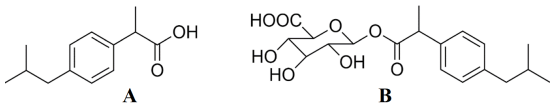

Figure 1 (**A**): Structure of ibuprofen; (**B**): ibuprofen β-D-glucuronide

Earlier, we investigated the elimination of racemic ibuprofen from the small intestine in hyperglycemic rats by HPLC-UV. In parallel, by cannulation of the bile duct, we investigated the excretion of the parent compound and its glucuronide conjugate into the bile. Unconjugated ibuprofen (**1**) and ibuprofen-β-D-glucuronide (**2**) were detected in the bile; however, no ibuprofen-glucuronide could be detected in the intestinal perfusate. Excretion of both ibuprofen and ibuprofen-β-D-glucuronide into the bile was decreased in experimental diabetes [8].

Continuing the above investigations, we report on HPLV-UV analysis of ibuprofen enantiomers in the intestinal perfusate and bile of the hyperglycemic rats. The work aimed to get data if experimental hyperglycemia can modify the enantiomeric composition of the racemic ibuprofen in the small intestinal perfusate and the bile in our previously applied animal model. The *ex vivo* model provides direct information on the fate of the absorbed drug in the liver [8]. Thus, the hyperglycemia-induced change in the enantioselective hepatic metabolism and/or transportation can be investigated before the drug can enter the systemic circulation.

2 Materials and methods

2.1 Chemicals

Racemic ibuprofen (IBP), (*S*)-(+)-ibuprofen, salicylic acid, streptozotocin (STZ), and naproxen sodium (NAP) were purchased from Sigma-Aldrich (Budapest, Hungary). All chemicals and reagents were analytical or HPLC grade. The standard isotonic perfusion medium had the following compositions (mM): NaCl 96.4, KCl 7.0, $CaCl_2$ 3.0, $MgSO_4$ 1.0, sodium phosphate buffer (pH 7.4) 0.9, Tris buffer (pH 7.4) 29.5, glucose 14.0, mannitol 14.0. Blood glucose level was checked with an AccuChek blood glucose meter (Roche).

2.2 Animals

Male Wistar rats (9–11 weeks old, weighing 250–300 g) were separated into two groups. Group I was the control, and Group II was diabetic animals (n = 4 each). Experimental diabetes was induced by a 65 mg/kg bw intravenous injection of streptozotocin (STZ) one week before the intestinal perfusion. Blood glucose levels were tested before the STZ treatment and starting the experiments. The average blood glucose level of the control animals was 6.7 $\pm$ 1.5 mM, while that of the STZ-treated rats was 23.4 $\pm$ 2.8 mM.

2.3 Intestinal perfusion procedure

The experiments were performed according to the protocol before [8–10]. The animals fasted for 18–20 h before the experiments; and then were anesthetized with an intraperitoneal injection of urethane (1.2 g/kg bw, i.p.). The abdomen was opened by a midline incision. A jejunal loop (length of the jejunal loop about 10 cm) was "in vivo" isolated and cannulated at its proximal and distal ends. Body temperature was maintained at 37°C using a heat lamp.

Perfusion through the lumen of the jejunal loop with an isotonic medium containing 250 μM racemic ibuprofen was carried out at a rate of 13 ml/min in a recirculation mode. Perfusate samples (250 μl) were collected at selected timepoints from the perfusion medium from the intestinal loop for 150 minutes. The initial volume of the perfusate was 15 ml, and its temperature was maintained at 37°C.

For parallel investigation of the biliary excretion, the bile duct was cannulated with PE-10 tubing. The bile outflow was collected in 15 minute-periods into tared Eppendorf tubes placed in ice. The collected samples were stored in a deep freezer until analysis. Bile flow was measured gravimetrically, assuming a specific gravity of 1.0 [11].

2.4 Sample preparation

Perfusate and bile samples were kept at room temperature for a short time to become defrost. The extraction technique applies the validated method published by Bonato et al. [12]. The sample volume (50 μl) was placed in an Eppendorf tube, and then 10 μl of NAP solution (250 μM) was added as an internal standard (IS). The mixture was acidified by 40 μl of hydrochloric acid (2 M) and extracted with 1.5 ml (3-times 0.5 ml) of a mixture of n-hexane and ethyl acetate (8:2 v/v). The mixture was vortexed for 30 seconds, centrifuged for 5 minutes at 3500 rpm, and the transparent upper layer separated. The combined organic extracts were evaporated under nitrogen at 40°C. The residue was reconstituted in 50 μl of the mobile phase.

2.5 Instrumentation and chromatographic conditions

HPLC-UV analysis of the perfusate and bile samples extracts was performed on an integrated Jasco HPLC (LC-4000) system equipped with a PDA detector, a quaternary HPLC pump, a degasser, an autosampler, a thermostated column compartment, and a PDA detector. Data were recorded and evaluated by ChromNAV Data System (Ver.2). Ibuprofen enantiomers were separated on a Kromasil 3-amylCoat RP (4.6 mm $\times$ 150 mm, 3 μm) chiral column with a Teknokroma (ODS cartridge, 1 cm x 0.32 cm) guard column. The mobile phase consisted of methanol/water/acetic acid (70:30:0.1 v/v). The run time was 30 minutes with a 0.5 ml/min flow rate and 10 μl injection volume. The temperature and the UV detector were set at 22°C and 220 nm, respectively. The analytical method is based on the Kromasil application note [13]. Identification of the separated peaks was made by determination of the retention time of (*S*)-(+)-ibuprofen and NAP salt as an internal standard (Figure 2).

2.6 Validation data of HPLC analyses

2.6.1 Specificity

Results were evaluated based on the chromatograms of extracts of blank perfusate and blank bile samples. The examined extracts didn't give a detectable chromatographic peak at the retention time of ((*R*)-IBP (**1**) t_R = 14.5 min, (*S*)-IBP (**2**) t_R = 16.72 min, and NAP (**3**) t_R = 20.3

min) of the perfused medium; and at the retention time of ((*R*)-IBP (**1**) t_R = 14.4 min, (*S*)-IBP (**2**) t_R = 16.61 min and NAP (**3**) t_R = 20.18 min) of the bile (Figure 3).

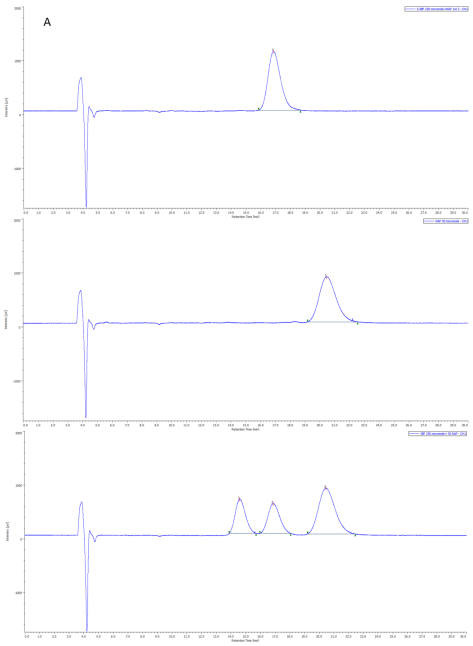

Figure 2 (**A**) HPLC-UV chromatogram of the (*S*)-IBP (t_R=16.85 min) in methanol, (**B**) the naproxen (t_R=20.44 min) in methanol, (**C**) the racemic IBP ((*R*)-ibuprofen (**1**) t_R=14.59 min, (*S*)-ibuprofen (**2**) t_R= 16.86 min) and naproxen (**3**) (t_R= 20.43 min) dissolved in the mobile phase.

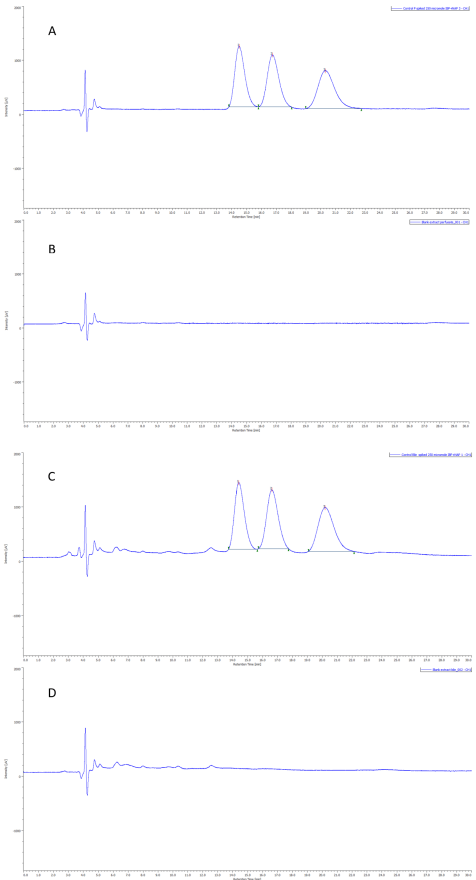

Figure 3 (**A**) HPLC-UV chromatogram of the two IBP enantiomers ((*R*)-IBP (**1**) t_R = 14.5 min, (*S*)-IBP (**2**) t_R = 16.72 min and NAP (**3**) t_R = 20.3 min), extracted from the spiked control perfusion medium of non-treated animal, (**B**) the blank control perfused medium, (**C**) the two IBP enantiomers ((*R*)-IBP (**1**) t_R = 14.4 min, (*S*)-IBP (**2**) t_R = 16.61 min and NAP (**3**) t_R = 20.18 min), extracted from the spiked control bile of non-treated animal; (**D**) the blank control bile.

2.6.2 System suitability

System suitability data were evaluated from chromatograms of the standard solutions of racemic IBP (100 μM, 250 μM) and NAP (50 μM) in methanol. Results were obtained from five parallel injections. The evaluation was based on the relative standard deviation (RSD%). The percent RSD values are shown in Table 1.

Table 1 Data for system suitability of methanol solutions of racemic ibuprofen (*rac*-IBP) (100 μM, 250 μM) and naproxen sodium (NAP) as internal standard (IS) (50 μM).

Injections (Standard Solutions)	NAP			rac-IBP				
	C (μM)	t_R(min)	Area	C (μM)	t_R(min)	R-Area	t_R(min)	S-Area
1	50	20.24	68666	100	14.48	12019	16.74	12119
2	50	20.22	68779	100	14.47	12081	16.72	12125
3	50	20.29	68783	100	14.50	12034	16.75	12156
4	50	20.30	68542	100	14.52	12034	16.79	12215
5	50	20.31	68632	100	14.53	12065	16.79	12247
Mean		20.27	68680		14.50	12047	16.76	12172
RSD%		0.17	0.13		0.16	0.19	0.17	0.41
Compounds	t_R	RRT	k'	T	NTP	R_S		
NAP	20.27	N/A	19.27	1.23	1567	N/A		
R-IBP	14.50	1.40	13.50	1.24	2057	1.63		
S-IBP	16.76	1.21	15.76	1.16	2009	1.99		
1	50	20.24	68740	250	14.47	32102	16.72	32200
2	50	20.24	68575	250	14.46	32121	16.70	32481
3	50	20.24	68552	250	14.46	32107	16.70	32272
4	50	20.24	68667	250	14.47	32096	16.71	32224
5	50	20.25	68244	250	14.48	31873	16.72	31979
Mean		20.24	68556		14.47	32060	16.71	32231
RSD%		0.03	0.25		0.03	0.29	0.04	0.50
Compounds	t_R	RRT	k'	T	NTP	R_S		
NAP	20.24	N/A	19.24	1.26	1522	N/A		
R-IBP	14.47	1.40	13.47	1.24	2057	1.63		
S-IBP	16.71	1.21	15.71	1.17	2026	1.99		

2.6.3 Precision

Precision was studied by investigating repeatability and intermediate precision. Repeatability was determined by measuring intra-day data of 3 parallel injections of 2 parallel dilutions of 2 independent weighings of racemic IBP (c = 100 μM, c = 250 μM in MeOH) and NAP (c = 50 μM, in MeOH). Intermediate precision was determined by measuring inter-day (by injection of the samples over three consecutive days) data of 3 parallel injections of 2 dilutions of racemic IBP (c = 100 μM, c = 250 μM in MeOH), and NAP (c = 250 μM, in MeOH). The evaluation was based on the relative standard deviation (RSD%) (Table 2 and 3).

Table 2 Data for system repeatability methanol solution of racemic ibuprofen (*rac*-IBP) (100 μM, 250 μM) and naproxen sodium (NAP) as internal standard (IS) (50 μM).

Weighting/Dilution Standard Solution	NAP		rac-IBP		
	C (μM)	Area	C (μM)	R-Area	S-Area
1/1	50	68358	250	31427	31471
1/2	50	68736	250	31612	31845
1/3	50	68381	250	31454	32084
2/1	50	68014	250	31765	32110
2/2	50	68568	250	31974	32247
2/3	50	68424	250	32123	32316
Mean		68414		31726	32012
RSD%		0.32		0.81	0.89
1/1	50	68901	100	12396	12362
1/2	50	68867	100	12124	12198
1/3	50	68882	100	12299	12442
2/1	50	68947	100	12284	12450
2/2	50	68993	100	12172	12268
2/3	50	68848	100	12288	12361
Mean		68906		12261	12347
RSD%		0.07		0.73	0.73

2.6.4 Accuracy

Accuracy was calculated by spiking control perfusion and bile samples with the concentrations of racemic IBP (50 μM, 100 μM, 250 μM) and NAP (50 μM). After the extraction of the samples, the percentage of recoveries was calculated with the mean of the same concentrations of standard dilutions of racemic IBP (50 μM, 100 μM, 250 μM) and NAP (50 μM). The evaluation was based on the relative standard deviation (RSD%) (Table 4).

Table 3 Data for system intermediate precision of methanol solution of racemic ibuprofen (rac-IBP) (100 μM, 250 μM) and naproxen sodium (NAP) as internal standard (IS) (50 μM).

Day	Dilution Standard Solution	NAP		rac-IBP		
		C (μM)	Area	C (μM)	R-Area	S-Area
1	1	50	68358	250	31427	31471
	2	50	68736	250	31612	31845
	3	50	68381	250	31454	32084
2	1	50	68313	250	31617	31781
	2	50	68687	250	31440	31686
	3	50	68747	250	31325	31546
3	1	50	68884	250	32130	32366
	2	50	68262	250	32055	32349
	3	50	68461	250	32052	32308
	Mean		68537		31679	31937
	RSD%		0.31		0.93	1.03
1	1	50	68901	100	12396	12362
	2	50	68867	100	12124	12198
	3	50	68882	100	12299	12442
2	1	50	68935	100	12355	12492
	2	50	68227	100	12065	12129
	3	50	68568	100	12207	12291
3	1	50	68905	100	12148	12246
	2	50	68859	100	12178	12315
	3	50	68714	100	12058	12375
	Mean		68762		12203	12317
	RSD%		0.32		0.94	0.88

Table 4 Accuracy of NAP, *R*- and *S*-IBP determination in spiked control perfusates and spiked control bile with the same range of standard dilutions of racemic IBP (50 μM, 100 μM, 250 μM) and NAP(50 μM).

	NAP			rac-IBP			
C_{SP} (μM)	Area	Recovery %	C_{SP} (μM)	R-Area	Recovery %	S-Area	Recovery %
50	67646	98.1	50	5299	86.5	5241	85.0
50	67599	98.0	50	5335	87.1	5299	85.9
50	67569	98.0	50	5320	86.8	5227	84.7
50	68004	98.4	100	11355	92.8	11248	90.9
50	67423	97.6	100	11151	91.1	11088	89.6
50	67536	97.7	100	11097	90.7	11006	88.9
50	56635	81.6	250	26897	85.7	26898	85.3
50	56225	81.1	250	26855	85.5	26741	84.8
50	55432	79.9	250	26361	83.9	26326	83.5
Mean		92.3			87.8		86.5
RSD%		8.76			3.23		2.81
C_{SB} (μM)	Area	Recovery %	C_{SB} (μM)	R-Area	Recovery %	S-Area	Recovery %
50	61456	89.1	50	5168	84.3	5164	83.7
50	61475	89.2	50	5127	83.7	5169	83.8
50	61466	89.2	50	5147	84.0	5166	83.8
50	60576	87.7	100	10930	89.3	11049	89.3
50	60411	87.4	100	10916	89.2	11003	88.9
50	60494	87.5	100	10923	89.3	11026	89.1
50	60968	87.9	250	28149	89.6	29544	93.7
50	61118	88.1	250	27995	89.2	28732	91.1
50	61043	88.0	250	28072	89.4	29138	92.4
Mean		88.2			87.6		88.4
RSD%		0.77			2.88		4.09

Note: SP: spiked perfusate; SB: spiked bile.

2.6.5 Linearity

Linearity was studied by analysis of standard solutions of racemic IBP of five different concentrations (250 μM, 200 μM, 150 μM, 100 μM, 50 μM) using methanol as solvent. Each solution had a known concentration of NAP as an internal standard (50 μM). Data were obtained from three parallel injections of each concentration. Calibration curves were generated by plotting the theoretical concentrations against the relative peak areas (ratio of the peak areas of the enantiomers and the internal standard). Linearity was determined by least-squares regression. The regression equation for (*R*)- and (*S*)-IBP was as follows: (*R*)-IBP: $y = 0.3360x + 0.2408$, $R^2 = 0.9993$; (*S*)-IBP: $y = 0.1676x + 0.2110$, $R^2 = 0.9994$) as shown in Figure 4.

2.6.6 Determination of LOQ

The limit of quantitation (LOQ) was considered the lowest concentration (50 μM) of the calibration curve contracted by using racemic ibuprofen. Taking into consideration the exact concentration of the two enantiomers in the investigated sample ((*R*)-IBP: 49.81%; (*S*)-IBP: 50.019% - See Table 1), the LOQ of the (*R*)-IBP and (*S*)-IBP are 24.91 μM and 25.09 μM, respectively.

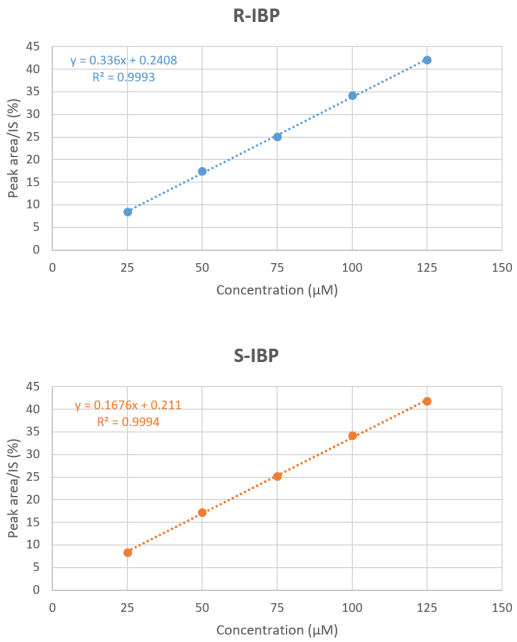

Figure 4 The HPLC-UV calibration curves of *R*-IBP (**A**) and *S*-IBP (**B**) with the linear regression trend lines, constructed by five different concentrations (250 μM, 200 μM, 150 μM, 100 μM, 50 μM) of standard racemic IBP.

2.7 Calculations and statistics

The luminal disappearance of the IBP enantiomers was calculated based on their luminal concentrations and the volume of the perfusion solution. The biliary excretion was calculated on the base of the volume of bile flow in 15 minutes periods. Data show the mean $\pm$ SD of four independent experiments. The difference among groups was determined by SPSS One-way Anova. Significant differences from the control value: * $p<0.05$, ** $p < 0.01$, and $_{***}$ $p < 0.001$.

2.8 Ethical approval

The study was designed and conducted according to the European legislation (Directive 2010/63/E.U.) [14] and the Hungarian Government regulation (40/2013., II. 14.) [15] on the protection of animals used for scientific purposes. The project was approved by the Animal Welfare Committee of the University of Pécs and by the Government Office of Baranya County (license No. BAI35/51-61/2016 and license supplement (supplement No. BAI35/90-5/2019).

3 Results

Figure 3(A) and 3(C) shows the HPLC-UV chromatograms of the two ibuprofen enantiomers and naproxen (used as internal standard) extracted from the control perfusion medium and the control bile, respectively. The blank control (buffer perfused through isolated small intestine of not treated rat) doesn't have any interfering peak (Figure 3(B)). The blank control bile (biliary excretion collected from the bile duct) doesn't have any interfering peak (Figure 3(D)).

HPLC chromatograms of the intestinal perfusates of the control and the STZ-treated (hyperglycemic) rats at the 0, 29, and 90-minute timepoints are shown in Figure 5 and Figure 6, respectively. Changes in concentrations of the IBP enantiomers in the perfusions of the control and hyperglycemic rats are shown in Figure 7. The relative amount of the (*S*)-IBP enantiomer in the control animals was slightly higher from the 22- to the 45-minute timepoints of the experiments; however, the difference cannot be assessed statistically (Figure 7(A)). Such a change couldn't be observed in the samples of the hyperglycemic rats (Figure 7(B)).

In the bile samples collected during the intestinal perfusion of racemic IBP, only the (*S*)-IBP enantiomer could be detected. HPLC chromatograms of bile samples of control and hyperglycemic rats at the 30, 60, and 120-minute timepoints are shown in Figure 8 and Figure 9, respectively. In the chromatograms, two unknown peaks also appeared. Based on their relative retention times (compared to the IS), none of them could be identified by the available standards (IBP, 1-, 2-, 3-OH-IBP, and IBP-GLU). The concentrations of the (*S*)-IBP enantiomer measured in the bile samples of control and hyperglycemic rats are shown in Figure 10. The biliary excretion (*S*)-IBP was statistically lower in the hyperglycemic (STZ-treated) animals.

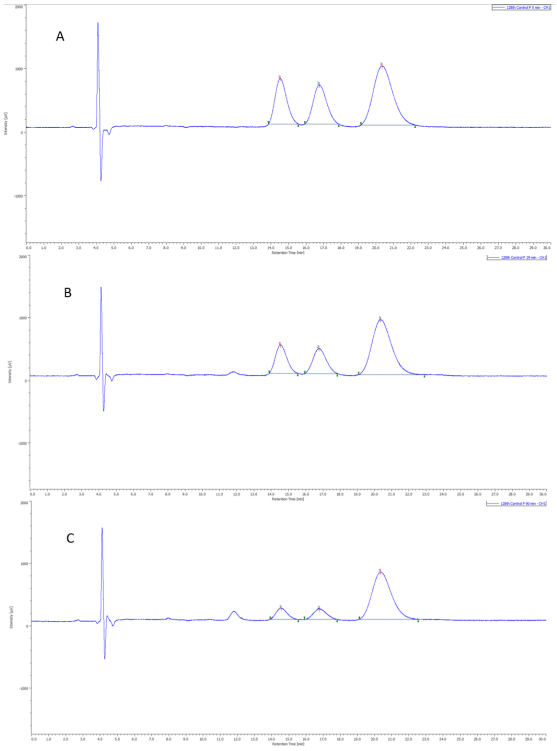

Figure 5 HPLC-UV chromatograms of extracts of intestinal perfusate of 250 μM racemic IBP spiked with 250 μM NAP (IS) at (**A**) 0-minute: (*R*)-IBP (**1**) (t_R=14.52 min), (S)-IBP (**2**) (t_R=16.75 min), NAP (**3**) (t_R=20.35 min); (**B**) 29-minute: (*R*)-IBP (**1**) (t_R=14.53 min), (*S*)-IBP (**2**) (t_R=16.76 min), NAP (**3**) (t_R=20.35 min); and (**C**) 90-minute: (*R*)-IBP (**1**) (t_R=14.54 min), (*S*)-IBP (**2**) (t_R=16.78 min), NAP (**3**) (t_R= 20.35 min) of control rats.

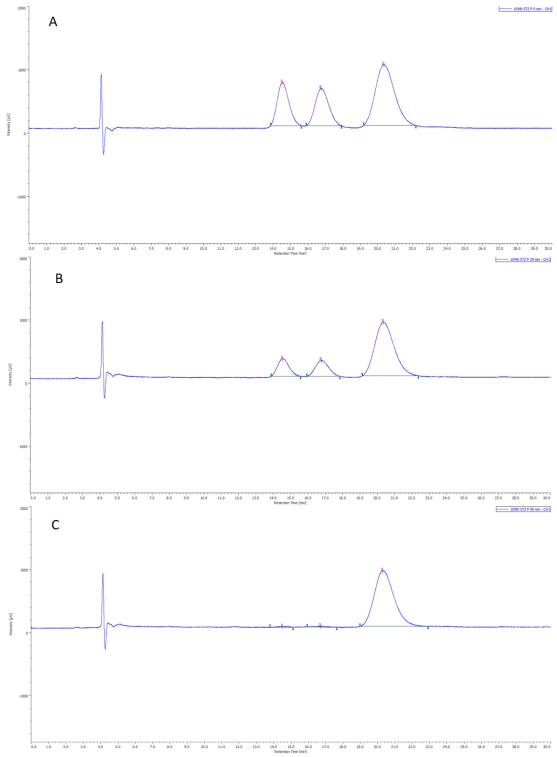

Figure 6 HPLC-UV chromatograms of extracts of intestinal perfusate of 250 μM racemic IBP spiked with 250 μM NAP (IS) at (**A**) 0-minute: (*R*)-IBP (**1**) (t_R=14.52 min), (S)-IBP (**2**) (t_R=16.75 min), NAP (**3**) (t_R= 20.35 min); (**B**) 29-minute: (*R*)-ibuprofen (**1**) (t_R=14.53 min), (S)-IBP (**2**) (t_R=16.76 min), NAP (**3**) (t_R=20.35 min); and (**C**) 90-minute: (*R*)-IBP (**1**) (t_R=14.51 min), (*S*)-IBP (**2**) (t_R=16.73 min), NAP (**3**) (t_R=20.31 min) of hyperglycemic rats.

The cumulative excretion of (*S*)-IBP in the extracts of the bile samples of control and hyperglycemic rats is shown in Figure 11. The cumulative excretion of the IBP enantiomer was statistically lower in the hyperglycemic rats.

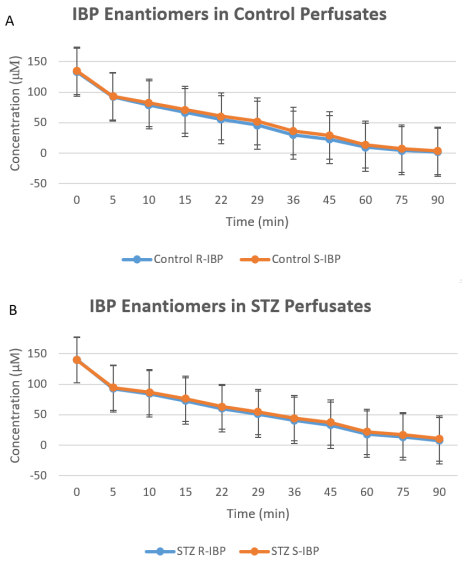

Figure 7 The concentrations of the IBP enantiomers in the extracts of the intestinal perfusates of the control (**7A**) and hyperglycemic (**7B**) rats (n = 4).

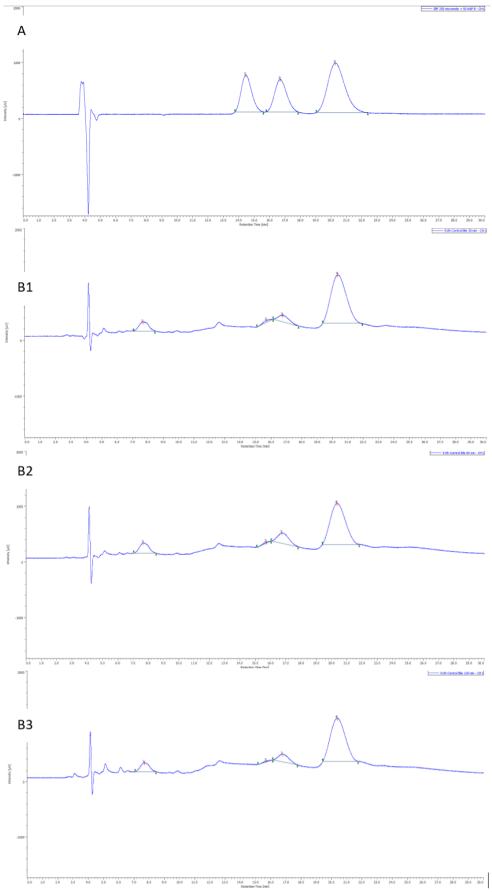

Figure 8 (**A**) HPLC-UV chromatogram of 250 μM of racemic IBP ((*R*)- (**1**) t_R=14.45 min, (*S*)-IBP (**2**) t_R=16.69 min) and NAP (**3**) (t_R=20.26 min) in the mobile phase; HPLC-UV chromatograms of bile extract at (**B1**) 30-minute: unknown peak (**1**) (t_R=7.68 min), unknown peak (**2**) (t_R=15.72 min), (*S*)-IBP (**3**) (t_R=16.75 min), NAP (**4**) (t_R=20.33 min); (**B2**) 60-minute: unknown peak (**1**) (t_R= 7.68 min), unknown peak (**2**) (t_R=15.72 min), (*S*)-IBP (**3**) (t_R= 16.76 min), NAP (**4**) (t_R=23.35 min); and (**B3**) 120-minute: unknown peak (**1**) (t_R=7.69 min), unknown peak (**2**) (t_R=15.72 min), (*S*)-IBP (**3**) (t_R=16.76 min), NAP (**4**) (t_R=20.36 min) of control rats.

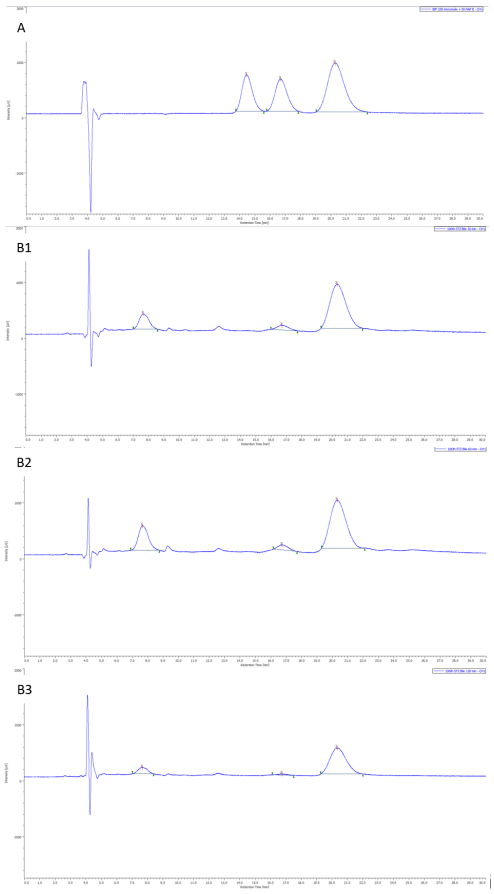

Figure 9 (**A**) HPLC-UV chromatogram of 250 mM of racemic IBP ((*R*)- (**1**) t_R=14.45 min, (*S*)-IBP (**2**) t_R=16.69 min) and NAP (**3**) (t_R=20.26 min) in the mobile phase; HPLC-UV chromatograms of excreted bile extract at (**B1**) 30-minute: unknown peak (**1**) (t_R=7.68 min), (*S*)-IBP (**2**) (t_R=16.72 min), NAP (**3**) (t_R=20.3 min); (**B2**) 60-minute: unknown peak (**1**) (t_R=7.66 min), (*S*)-IBP (**2**) (t_R=16.73 min), NAP (**3**) (t_R=20.31 min); and (**B3**) 120-minute: unknown peak (**1**) (t_R=7.66 min), (*S*)-IBP (**2**) (t_R=16.75 min), NAP (**3**) (t_R=20.32 min) of hyperglycemic rats.

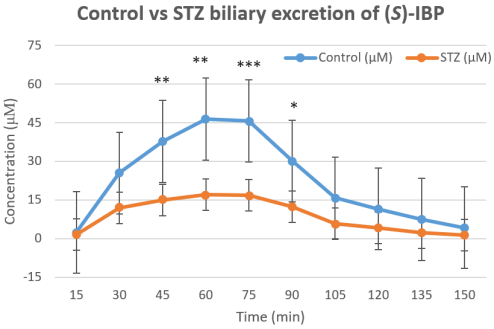

Figure 10 The concentration of (*S*)-IBP in the extracts of the bile samples of control and hyperglycemic animals (n = 4). Significant differences from the control value: * $p < 0.05$, ** $p < 0.01$, and *** $p < 0.001$.

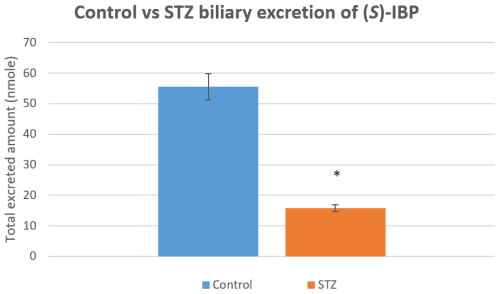

Figure 11 The cumulative excretion of (*S*)-IBP enantiomer in the extracts of the bile samples of control and hyperglycemic rats (n = 4); Significant differences from the control value: * $p < 0.01$.

4 Discussion

As shown in Figure 7A and 7B, the concentration of the two IBP enantiomers was continuously decreased in the intestinal perfusion medium over the experiments. (In the samples collected between the 105-150 min timepoints, IBP peaks could not be quantified. Legen et al. demonstrated that the inwardly directed proton gradient could be a driving force for transporting monocarboxylic acid-type drugs (among them IBP) across the intestinal epithelia [16]. The passive diffusion of the compound can explain the gradual decrease of concentration of the ibuprofen enantiomers in the perfusate.

Disappearance (absorption, metabolism, and excretion) of both enantiomers of IBU was lower in the hyperglycemic rats (Figure 7A and 7B); however, the change was statistically insignificant. Several reports have demonstrated that diabetes may decrease P-gp (MDR1) efflux transporter function and expression in the brain and the intestine [17–20]. In addition, curcumin and ibuprofen were reported to inhibit the P-gp activity of human sarcoma MES-SA/Dx-5 cells well below their therapeutic plasma concentrations [21]. P-gp effluxes drug substrates from enterocytes into the GI lumen, thus regulating the intestinal absorption of drugs. It is still unclear, however, which, if any, transporters facilitate the uptake or efflux of ibuprofen *in vivo*. It is a weak acid and is lipid soluble; hence, it is feasible that it may be able to cross membranes without the need for specific transporters [1].

In the bile samples, only the (*S*)-ibuprofen enantiomer could be detected (Figure 8 and 9). Figure 11 shows that the excreted amount of (*S*)-IBP is statistically lower in the bile samples of the hyperglycemic rats. Uptake transporters are expressed highly on the basolateral membrane of hepatocytes [22, 23]. The organic anion transporters hOAT1-5 are predominantly expressed in renal proximal tubules; however, hOAT2 (Slc22a7) is also expressed in the liver [24–26]. In the rat, the main site of expression of Oat2 is the sinusoidal membrane domain of the hepatocytes [27]. Kimoto et al. evaluated the role of organic anion transporter 2 (OAT2)-mediated hepatic uptake in the clearance of 25 ECCS Class 1A drugs. The authors provided evidence for the role of OAT2-mediated hepatic uptake of most of the investigated ECCS 1A drugs, including IBP [28]. Members of the organic anion transporting polypeptide (OATP) family are also important determinants of hepatic uptake of endogenous and exogenous compounds. Kindla et al. reported that only diclofenac was significantly transported by OATP1B3, whereas all other NSAIDs investigated (including IBP) were not substrates for these uptake transporters [29]. Accordingly, ibuprofen is supposed to enter the hepatocytes by passive diffusion and OATP2-mediated uptake [1, 28, 30].

Schneider et al. investigated the biliary elimination of ibuprofen, indomethacin, and diclofenac in patients suffering from obstructions of the common bile duct. Whereas a very low amount (0.15%) of ibuprofen was excreted in bile as unchanged drug and active conjugates, biliary elimination of diclofenac was somewhat higher (1.09%), and that of indomethacin was substantial (above 10%) [31]. Like the small intestine, the P-gp efflux transporter (Mdr1) is also expressed in the apical side of the rat hepatocytes [22]. P-gp has been reported to be reduced in hyperglycemic rats [18, 19, 32]. Using the present experimental protocol (entering the total amount of absorbed IBP in the bile through the vena portae), we found a relatively low amount of (non-enantiomer-separated) IBP and IBP-glucuronide in the bile. The biliary appearance of both compounds was depressed under hyperglycemic conditions. Our molecular biology studies on liver samples of the STZ-treated rats showed decreased expression of the efflux transporters P-gp (Mdr1B), Mrp2, and Bcrp [8]. These transporters are involved in exporting organic anions from the hepatocytes into the bile canaliculus [33].

Biliary excretion of the parent compounds and their metabolites is crucial for the so-called enterohepatic circulation of the drugs and other xenobiotics [34]. Drugs in bile are usually more concentrated than in plasma, and passive transport is considered negligible. Accordingly, biliary excretion represents an active process involving transporters embedded in the apical membrane of hepatocytes. Furthermore, the liver was the most important organ in the unidirectional conversion of (*R*)-arylpropionic acid drugs to their (*S*) enantiomer. Whether the asymmetric appearance of the IBP enantiomers is the consequence of the OAT2-mediated enantioselective hepatic uptake or the enantioselective excretion of the hepatic efflux transporters P-gp (Mdr1B), Mrp2, and Bcrp (or both) needs further molecular biology studies.

5 Conclusions

This study provided experimental data on intestinal elimination and hepatic excretion of the IBP enantiomers in control and hyperglycemic experimental animals. The results demonstrated that the elimination of IBP from the small intestine is not enantioselective. Analysis of the bile showed the presence of only the pharmacologically more active (*S*)-IBP enantiomer. Since the

pharmacological activity of (*S*)-IBP is one order of magnitude higher than that of the (*R*)-IBP [35], the asymmetric appearance of the enantiomers in the bile could determine the pharmacokinetics and pharmacodynamic action of the drug.

Conflict of interest

None of the authors declared a conflict of interest.

Funding

This study was supported by the European Union and co-financed by the European Social Fund (EFOP-3.6.1.-16-2016-00004). The financial support is highly appreciated.

Author contributions

Conceptualization (P.P.), Investigation (H.O.M., A.A.), Methodology (P.P., H.O.M., A.A.), Writing – original draft (P.P. and H.O.M.), Writing – review, and editing (P.P. and H.O.M.), Funding acquisition (P.P.). All authors have read and agreed to the published version of the manuscript.

Abbreviations

STZ	Streptozotocin
HPLC	High performance liquid chromatography
UV	Ultraviolet
NSAID	Non-steroidal anti-inflammatory drug
IBP	Ibuprofen
NAP	Naproxen sodium salt
IS	Internal standard
MeOH	Methanol
SD	Standard Deviation
RSD	Relative Standard Deviation
MDR1/P-gp	Multidrug resistance protein 1/P-glycoprotein
OAT	Organic anion transporters
OATP	Organic anion transporting polypeptide
MRP2	Multidrug resistance-associated protein 2
BCRP	Breast cancer resistance protein
PDA	Photodiode array

References

[1] Mazaleuskaya LL, Theken KN, Gong L, *et al*. PharmGKB summary: Ibuprofen pathways. Pharmacogenetics and Genomics, 2015, **25**: 96-106. https://doi.org/10.1097/FPC.0000000000000113

[2] Rudy AC, Knight PM, Brater DC, *et al*. Stereoselective metabolism of ibuprofen in humans: administration of R-, S- and racemic ibuprofen. The Journal of Pharmacology and Experimental Therapeutics, 1991, **259**: 1133-1139. https://doi.org/10.0000/PMID1762067

[3] Brocks D and Jamali F. The pharmacokinetics of ibuprofen in humans and animals. In: Rainsford KD (ed), Ibuprofen. A critical bibliographic review. Taylor & Francis, London, 1999, 89-142.

[4] Jeffrey P, Tucker GT, Bye A, *et al*. The site of inversion of R(-)-ibuprofen: studies using rat in situ isolated perfused intestine/liver preparations. Journal of Pharmacy and Pharmacology, 1991, **43**: 715-720. https://doi.org/10.1111/j.2042-7158.1991.tb03464.x

[5] Jamali F, Mehvar R, Russell AS, *et al*. Human pharmacokinetics of ibuprofen enantiomers following different doses and formulations: intestinal chiral inversion. Journal of Pharmaceutical Sciences, 1992, **81**: 221-225. https://doi.org/10.1002/jps.2600810306

[6] Keep DR, Sidelmann UG and Hansen SH. Isolation and characterization of major phase I and II metabolites of ibuprofen. Pharmaceutical Research, 1997, **14**: 676-680. https://doi.org/10.1023/A:1012125700497

[7] Rainsford KD. Ibuprofen: pharmacology, efficacy and safety. Inflammopharmacology, 2009, **17**: 275-342. https://doi.org/10.1007/s10787-009-0016-x

[8] Kovács NP, Almási A, Garai K, *et al*. Investigation of intestinal elimination and biliary excretion of ibuprofen in hyperglycemic rats. The Canadian Journal of Physiology and Pharmacology, 2019, **97**: 1080-1089. https://doi.org/10.1139/cjpp-2019-0164

[9] Fischer E, Almási A, Bojcsev S, *et al*. Effect of experimental diabetes and insulin replacement on intestinal metabolism and excretion of 4-nitrophenol in rats. The Canadian Journal of Physiology and Pharmacology, 2015, **93**: 459-464.
https://doi.org/10.1139/cjpp-2015-0065

[10] Almási A, Perjési P and Fischer E. The relative importance of the small intestine and the liver in Phase II metabolic transformations and elimination of p-nitrophenol administered in different doses in the rat. Scientia Pharmaceutica, 2020, **88**: 512020.
https://doi.org/10.3390/scipharm88040051

[11] Klaassen CD. Bile flow and bile composition during bile acid depletion and administration. Canadian journal of physiology and pharmacology, 1974, **52**: 334-348.
https://doi.org/10.1139/y74-045

[12] Bonato PS, Del Lama MPFM and de Carvalho R. Enantioselective determination of ibuprofen in plasma by high-performance liquid chromatography–electrospray mass spectrometry. Journal of Chromatography B, 2003, **796**: 413-420.
https://doi.org/10.1016/j.jchromb.2003.08.031

[13] Kromasil Application Note, n.d., viewed September 28, 2022.
https://www.kromasil.com/applications/view.php?app=c0128

[14] European legislation (Directive 2010/63/E.U.). viewed September 28, 2022.
https://eur-lex.europa.eu/eli/dir/2010/63/oj

[15] Hungarian Government regulation (40/2013., II. 14.) viewed September 28, 2022.
https://www.fao.org/faolex/results/details/en/c/LEX-FAOC124420

[16] Legen I, Zakelj S and Kristl A. Polarised transport of monocarboxylic acid type drugs across rat jejunum in vitro: the effect of mucolysis and ATP-depletion. International Journal of Pharmaceutics, 2003, **256**: 161-166.
https://doi.org/10.1016/s0378-5173(03)00073-5

[17] Liu H, Xu X, Yang Z, *et al*. Impaired function and expression of P-glycoprotein in blood-brain barrier of streptozotocin-induced diabetic rats. Brain Research, 2006, **1123**: 245-252.
https://doi.org/10.1016/j.brainres.2006.09.061

[18] Nawa A, Fujita Hamabe W and Tokuyama S. Inducible nitric oxide synthase-mediated decrease of intestinal P-glycoprotein expression under streptozotocin-induced diabetic conditions. Life Sciences, 2010, **86**: 402-409.
https://doi.org/10.1016/j.lfs.2010.01.009

[19] Zhang L, Lu L, Jin S, *et al*. Tissue-specific alterations in expression and function of P-glycoprotein in streptozotocin-induced diabetic rats. Acta Pharmacologica Sinica, 2011, **32**: 956-966.
https://doi.org/10.1038/aps.2011.33

[20] Drozdzik M, Czekawy I, Oswald S, *et al*. Intestinal drug transporters in pathological states: an overview. Pharmacological Reports, 2020, 72: 1173-1194.
https://doi.org/10.1007/s43440-020-00139-6

[21] Angelini A, Lezzi M, di Febbo C, *et al*. Reversal of P-glycoprotein-mediated multidrug resistance in human sarcoma MES-SA/Dx-5 cells by nonsteroidal anti-inflammatory drugs. Oncology Reports, 2008, **20**: 731-735.
https://doi.org/10.3892/or_00000067

[22] Klaassen CD and Aleksunes LM. Xenobiotic, bile acid, and cholesterol transporters: function and regulation. Pharmacological Reviews, 2010, **62**(1): 1-96.
https://doi.org/10.1124/pr.109.002014

[23] Burckhardt G. Drug transport by Organic Anion Transporters (OATs). Pharmacology & Therapeutics, 2012, **136**: 106-130.
https://doi.org/10.1016/j.pharmthera.2012.07.010

[24] Cha SH, Sekine T, Fukushima JI, *et al*. Identification and characterization of human organic anion transporter 3 expressing predominantly in the kidney. Molecular Pharmacology, 2001, **59**: 1277-1286.
https://doi.org/10.1124/mol.59.5.1277

[25] Kobayashi Y, Ohshiro N, Sakai R, *et al*. Transport mechanism and substrate specificity of human organic anion transporter 2 (hOat2 [SLC22A7]). Journal of Pharmacy and Pharmacology, 2005, **57**: 573-578.
https://doi.org/10.1211/0022357055966

[26] Nigam SK, Bush KT, Martovetsky G, *et al*. The organic anion transporter (OAT) family: A systems biology perspective. Physiological Reviews, 2015, **95**: 83-123.
https://doi.org/10.1152/physrev.00025.2013

[27] Fork C, Bauer T, Golz S, *et al*. OAT2 catalyses efflux of glutamate and uptake of orotic acid. The Biochemical Journal, 2011, **436**: 305-312.
https://doi.org/10.1042/BJ20101904

[28] Kimoto E, Mathialagan S, Tylaska L, *et al*. Organic anion transporter 2–mediated hepatic uptake contributes to the clearance of high-permeability–low-molecular-weight acid and zwitterion drugs: Evaluation using 25 drugs. The Journal of Pharmacology and Experimental Therapeutics, 2018, **367**: 322-334.
https://doi.org/10.1124/jpet.118.252049

[29] Kindla J, Müller F, Mieth M, *et al*. Influence of non-steroidal anti-inflammatory drugs on organic anion transporting polypeptide (OATP) 1B1- and OATP1B3-mediated drug transport. Drug Metabolism and Disposition, 2011, **39**: 1047-1053.
https://doi.org/10.1124/dmd.110.037622

[30] Davies NM. Clinical pharmacokinetics of ibuprofen. The first 30 years. Clinical Pharmacokinetics, 1998, **34**: 101-154.
https://doi.org/10.2165/00003088-199834020-00002

[31] Schneider HT, Nuernberg B, Dietzel K, *et al*. Biliary elimination of non-steroidal anti-inflammatory drugs in patients. British Journal of Clinical Pharmacology, 1990, **29**: 127-131.
https://doi.org/10.1111/j.1365-2125.1990.tb03613.x

[32] Anger GJ, Magomedova L and Piquette-Miller M. Impact of acute streptozotocin-induced diabetes on ABC transporter expression in rats. Chemistry and Biodiversity, 2009, **6**: 1943-1959.
https://doi.org/10.1002/cbdv.200900053

[33] Jetter A and Kullak-Ublick GA. Drugs and hepatic transporters: A review. Pharmacological Research, 2020, **154**: 104234.
https://doi.org/10.1016/j.phrs.2019.04.018

[34] Yang X, Gandhi YA, Duignan DB, *et al*. Prediction of biliary excretion in rats and humans using molecular weight and quantitative structure–pharmacokinetic relationships. The AAPS Journal, 2009, **11**: 511-525.
https://doi.org/10.1208/s12248-009-9124-1

[35] Neupert W, Brugger R, Euchenhofer C, *et al*. Effects of ibuprofen enantiomers and its coenzyme A thioesters on human prostaglandin endoperoxide synthases. British Journal of Clinical Pharmacology, 1997, **122**: 487-492.
https://doi.org/10.1038/sj.bjp.0701415